

LiDAR and SfM-MVS Integrated Approach to Build a Highly Detailed 3D Virtual Model of Urban Areas

Original

LiDAR and SfM-MVS Integrated Approach to Build a Highly Detailed 3D Virtual Model of Urban Areas / Grasso, Nives; Spadavecchia, Claudio; Belcore, Elena; Di Pietra, Vincenzo. - ELETTRONICO. - (2023), pp. 128-135. (9th International Conference on Geographical Information Systems Theory, Applications and Management Praga 24-27 Aprile 2023) [10.5220/0011760800003473].

Availability:

This version is available at: 11583/2978268 since: 2023-05-02T09:30:45Z

Publisher:

International Conference on Geographical Information Systems Theory, Applications and Management

Published

DOI:10.5220/0011760800003473

Terms of use:

This article is made available under terms and conditions as specified in the corresponding bibliographic description in the repository

Publisher copyright

(Article begins on next page)

LiDAR and SfM-MVS Integrated Approach to Build a Highly Detailed 3D Virtual Model of Urban Areas

Nives Grasso^a, Claudio Spadavecchia^b, Vincenzo Di Pietra^c and Elena Belcore^d

DIATI, Politecnico di Torino, Corso Duca degli Abruzzi 24, 10129 Torino, Italy

nives.grasso@polito.it, claudio.spadavecchia@polito.it, vincenzo.dipietra@polito.it, elena.belcore@polito.it

Keywords: 3D Models, Multisensor, Multiscale, LiDAR, UAS, Data Integration, Data Fusion, Geomatics.

Abstract: The three-dimensional reconstruction of buildings, road infrastructures, service networks, and cultural heritage in urban environments is relevant for many market segments and numerous functions in the management and coordination of public authorities. These stakeholders are showing increasing interest in modern acquisition and reconstruction technologies for digital models typical of the geomatic and computer vision disciplines. In this context, it is essential to methodically exploit the potential of active and passive instruments and apply multi-sensor integration techniques, to obtain metrically accurate and high-resolution products. This study proposes a multi-sensor and multi-scale approach for high-resolution 3D model reconstruction focused on a city portion of Turin (Italy). We performed an integrated survey based on LiDAR and photogrammetric techniques, both aerial and terrestrial. Then we produced a set of 3D digital products for (i) promoting the historical and artistic heritage through Virtual Reality (VR) applications, (ii) supporting the restoration of Baroque buildings, and (iii) providing advanced analysis concerning the alteration of the urban road system. The final output describes in detail the architectural elements investigated (e.g., 9,480,000 triangles to define the mesh of a statue). It emphasizes the need for deepening sensor integration and data fusion.


1 INTRODUCTION


A virtual three-dimensional (3D) model of an urban environment is a computerised model of the urban environment in a three-dimensional geometry focusing on common urban objects and structures (Billen et al., 2014; Zhu et al., 2009). 3D modelling is a process that starts from data acquisition and ends with the final 3D virtual model (Remondino & El-Hakim, 2006); from this perspective, geomatic techniques such as Photogrammetry and Remote Sensing play a key role in creating a virtual 3D model of urban environments to the extent that they can be now considered as one of the most important and attractive products of the techniques mentioned above (Singh et al., 2013; Zhu et al., 2009).


From a general point of view, 3D models are generated (i) with aerial and/or terrestrial images (Remondino & El-Hakim, 2006; Sato et al., 2003)


with Structure from Motion/Multi-View Stereo (SfM-MVS) workflows (Pepe et al., 2022; Smith et al., 2016; Westoby et al., 2012); (ii) from point clouds acquired from terrestrial (TLS) and/or airborne (ALS) laser scanning (Tse et al., 2008; C. Wang et al., 2020); (iii) with an integrated approach using both images and point cloud data (El-Hakim et al., 2004; Ramos & Remondino, 2015; Sahin et al., 2012).

The image-based methodology is probably the most common approach thanks to the cheapness of the instrumentation required and the diffusion of Uncrewed Aerial Systems (UAS), also referred to as Unmanned Aerial Vehicles (UAV), for integrating aerial photos (Kobayashi, 2006). While large-scale three-dimensional models can be extracted using high-resolution satellite images (Kocaman et al., 2006), close-range images (combined terrestrial and UAS images) are used for more detailed reconstructions (Püschel et al., 2008; J. Wang & Li, 2007; Yalcin & Selcuk, 2015).

^a  <https://orcid.org/0000-0002-9548-6765>

^b  <https://orcid.org/0000-0003-2087-9828>

^c  <https://orcid.org/0000-0001-7501-1183>

^d  <https://orcid.org/0000-0002-3592-9384>

On the other hand, recent LiDAR (Light Detection And Ranging) technologies have become a valuable source for acquiring very dense data, which can be used to automatically extract urban elements like buildings, trees, and roads (Rottensteiner et al., 2005). The integrated approach became popular in the last few years, and nowadays, it is often preferred to the photogrammetric process. Data integration enhances the positive aspects of the two methodologies, compensating for both limits (Nex and Rinaudo 2011); the ease of use and affordability of the image-based approach complements the high accuracy obtained through the large amount of data acquired with a laser scanner. The result is a complete high-resolution 3D model with RGB information.

The high resolution of the virtual models that can be achieved translates into greater usability of the model themselves, as they can be applied in several domains (Biljecki et al., 2015). 3D models can be used to allow viewing and virtual navigation to support the preliminary planning phase of urban planning (Chen, 2011) and for dissemination, tourism, and information purposes. Models with higher resolution can be used for architectural (Chiabrando et al., 2019) and multi-temporal (Rodríguez-González et al., 2017) analysis in the cultural heritage research field and the Smart Cities domain (Jovanović et al., 2020). Many multi-scale and multi-sensor methods for large-scale detailed 3D city models and urban environment generation have been proposed; nonetheless, an established and shared workflow still does not exist.

In this study, we describe a well-defined framework for building high-resolution and large-scale 3D models by the integration of multi-scale and multi-sensor approaches and technologies, proposing an application generating a 3D model obtained with a LiDAR and photogrammetric integrated approach which describes a city portion of Turin (Italy), specifically Carlo Alberto Square, Carignano Square, Carignano Palace, and Po Street. The fields of interest of a three-dimensional and computerized city reconstruction thus obtained are diverse and include (i) the usability in Virtual Reality (VR) applications, allowing to enhance and promote the heritage of historical and artistic interest of the surveyed area with tourists, educational and didactic purposes; (ii) the monitoring and the restoration of historical (in this case Baroque) buildings, particularly complex due to their curvilinear style and rich in decorative elements; (iii) the support for advanced structural analyses concerning the alteration and the improvement of the urban road system (in the surveyed area a new metro stop will be constructed).

A multi-sensor and multi-scale approach was adopted to address the challenging nature of the diversity of purposes: the high-resolution survey performed with a laser scanner was integrated by the photogrammetric drone survey to model the roofs and the upper part of the buildings, while terrestrial photogrammetric acquisitions were necessary to improve the generation of the texture. Moreover, a further challenge was found in using the terrestrial laser scanner in an urban environment due to the constant flow of people (Lemmens, 2011), causing the generation of a noisy point cloud that had to be filtered during the processing phase.

To generate a high-resolution 3D model that can be used for the mentioned aims and at the same time allow ease of use and visualization by non-expert users and with less performing machines; it was decided to preserve higher resolutions only for the main buildings (Carignano Palace and Carlo Alberto Square).

2 CASE STUDY

The survey area extends for about 21,000 m² in a location of historical and architectural interest in Turin. The area includes Carignano Square, Carignano Palace, Carlo Alberto Square, Principe Amedeo Street and Cesare Battisti Street (in the extension between Carignano Square and Carlo Alberto Square), Carlo Alberto Street (between Carlo Alberto Square and Po Street) and Po Street (between Castello Square and Giambattista Bogino Street) (Figure 1).

The creation of a high-resolution 3D model was required: (i) to provide support for the renovation of Carlo Alberto Square, where a station for the new underground city metro line will be realized; (ii) to measure the exact location of the statue dedicated to Carlo Alberto (placed in the homonymous square) which, to preserve its integrity, will be removed during the construction phase and subsequently placed back in the exact location; (iii) to carry out further analyses concerning possible road interferences between the surface road network (in particular public transport by rail) and the planned underground road; (iv) to be used for virtual reality purposes, with particularly high detail for Carlo Alberto's statue and the facades of Carignano Palace; (v) interactively advertise citizens and tourists, through virtual reality navigation, about the inclusion of this road infrastructure work in an urban area of great historical, architectural and artistic interest, enhancing its beauty.

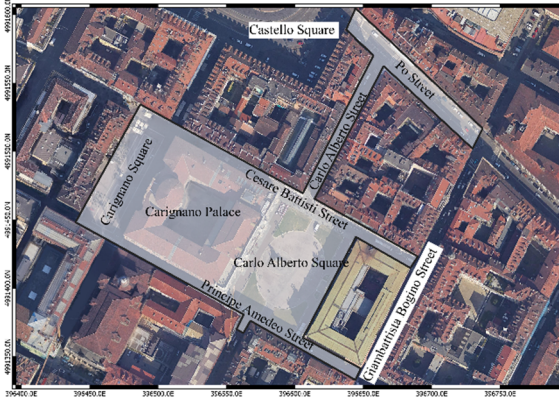


Figure 1: Study area. EPSG: 32632.

3 MATERIALS AND METHODS

3.1 Multi-Sensor and Multi-Scale Approach

A compromise between time spent on the data acquisition and data processing is the main challenge in generating a high-detail multi-scale and multi-purpose city 3D model. Therefore, the relation between area-to-be-surveyed and time-to-be-spent and the choice of sensors requires deep analysis since the selected sensors must ensure sufficient detail according to the survey purposes. As a result, it is necessary to use different sensors (multi-sensor approach) and consider different levels of detail (multi-scale approach) to meet these requirements. In the surveyed area, some objects have primary interest (Carignano Palace facade, Carlo Alberto's statue) respect to others (buildings in Cesare Battisti and Principe Amedeo Streets).

Hence, to strike a balance between the resolution requirements and the available resources, both optical and LiDAR sensors were considered. In detail, the sensors that were used are a Terrestrial Laser Scanner (TLS), a UAS-embedded optical sensor, a Nikon mirrorless camera, and a 360° portable sensor (Ricoh) (Table 1).

The LiDAR survey was carried out using a Riegl VZ-400i laser scanner combined with a Nikon D800 digital camera which aims to capture RGB images to color the point cloud. The laser scanner is also equipped with a GNSS antenna and an inertial platform integrated into the instrument.

Furthermore, a georeferencing system was established by integrating a Global Navigation Satellite System (GNSS)-acquired network thickened with reference stations and detailed with

retroreflecting markers and natural points. The natural points were distributed within the test area and acquired by a Total Station (TS) to obtain a reliable network of control and checkpoints.

Table 1: Specifications and purpose within the survey of the sensors.

| Sensor | Characteristics | | Purpose |
|----------------|--------------------|---------------------|---|
| DJI Mini Mavic | Resolution | 12 Mpx | Roofs modelling |
| | Focal Length | 4 mm | |
| | Sensor | 1/2.3" CMOS | |
| RIEGL VZ-400i | Measure technique | ToF | High-detailed reconstruction of facade geometries |
| | Operative distance | 0.5 – 800 m | |
| | FOV | 100°/360° | |
| | Frequency | 100/1200 Hz | |
| | Accuracy | 5/3 mm | |
| | Size | 206x308 mm | |
| NIKON D800E | Resolution | 36.2 Mpx | High-detailed texture generation |
| | Focal Length | 60 mm | |
| | Sensor | 35,9 x 24,0 mm CMOS | |
| Ricoh Theta V | Resolution | 12 Mpx (x2) | Texture generation for narrow streets |
| | Focal Length | 1 mm | |
| | Sensor | 1/2.3 CMOS(x2) | |

Due to moving elements and architectonic complexities, Carignano Square and Po Street are the most challenging areas to survey. Because of this, concern was raised about: (i) the planning of the UAS flight, for which it was necessary to take into account the proper overlap, the correct resolution, the adequate camera orientation, the best acquisition time to minimise shadows on facades, and the safety requirements related to the high tourist activity of the area; (ii) the location, the number and the resolution of TLS scans necessary to obtain a continuous surface with homogeneous point density; (iii) the methodology for the acquisition of the photo for the texture reconstruction constrained by the illumination conditions of the facades.

3.2 Topographic Network and Survey of Detail

The topographic survey aims to define a standard reference coordinate system for harmonising data gathered by different sensors and during separate acquisition sessions. A topographic network was materialised by four vertices and set up to ensure sufficient satellite visibility. The coordinates of the vertices were measured with GNSS instrumentation in rapid-static mode with 1-hour stationing for each point. The instruments used for GNSS surveys were the Leica GS14 and GS18, the dual frequency (L1 and L2) receivers that receive the GPS and GLONASS constellations.

GNSS data were post-processed in relative mode, using the data of the GNSS Interregional Positioning Service (SPIN 3 GNSS) permanent network in LGO (Leica Geo Office) software. The UTM-WGS84 projection was chosen as the reference cartographic grid. However, a conventional local isometric system (MTL2 ISO250) was adopted to avoid the typical deformations of cartographic representations. The GNSS heights were measured above the ellipsoid and converted into orthometric heights using the geoid undulations model “ITALGEO2005” provided by the Italian Geographic Military Institute (Istituto Geografico Militare, IGM).

Starting from the reference network, we acquired the position of some reference points using the total station Leica Geosystem Image Station and prisms, creating a polygonal scheme consisting of 14 station points. Several circular retroreflective artificial targets (5 cm radius) were placed along the facades and measured with the total station (Figure 2). These targets are easily identifiable within the LiDAR point clouds through the reflectivity information. Similarly, some easily distinguishable natural points were also measured (Figure 2). A total of 264 points were measured to allow georeferencing LiDAR and photogrammetric acquisitions.

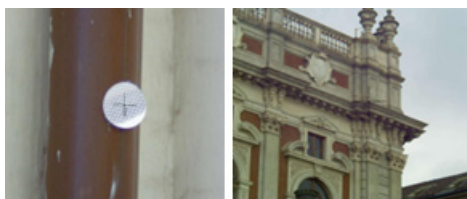


Figure 2: Example of a retroreflective target used during measurements (left) and natural point (right).

The compensation to the least squares of the network was performed through MicroSurvey Star*Net software, with a resulting standard deviation (RMSE) of the estimated coordinates less than 1 cm. Some Ground Control Points (GCPs) were materialised and measured with the GNSS receivers to georeference the UAS photogrammetric products. The measurements were conducted using NRTK-GNSS with centimetric precisions in real-time, thanks to the corrections from a local network of permanent SPIN 3 GNSS service stations. For this purpose, photographic points easily identifiable in drone images (e.g., edges of pavements, road markings, corners of maintenance holes) were exploited.

The coordinates acquired in the field were exported using LGO software to obtain the final coordinates in the national geodetic reference system ETRF2000 with 32N UTM projection.

3.3 The Terrestrial Lidar Acquisitions

A complete representation of the study area was obtained by performing 42 LiDAR scans acquired with an acquisition frequency of 600 kHz (acquisition speed of about 250000 points/second) and an angular resolution such that to obtain a point approximately every 6 mm at a distance of 10 m from the station point.

The data collected by the laser scanner and the topographic survey were post-processed using Riegl’s RiScan Pro software. The retroreflective targets were used for the relative registration of scans and their georeferencing in the absolute coordinate system. Each target was associated with the actual coordinates measured during the topographic survey. The scanning positions are firstly registered semi-automatically based on the Voxel analysis. The targets identified in the scans are used as additional observations for relative registration between scans to improve the estimation of scan locations. Then, the relative registration between scans and the georeferencing is further optimised considering all acquisitions made, as well as the available targets, the GNSS measurements, and the altitude measurements derived from the inertial platform. The optimisation phase also involves extracting the flat patches that characterise the surfaces of the represented environment from every scan. Subsequently, homologous planes between different scans and their correspondence are sought through an iterative process. At the end of this procedure, the relative position between the scans is permanently corrected. At the same time, the absolute position of the scans is estimated.

Raw scan data generally does not contain radiometric information but only information about the material's reflectivity. The Riegl VZ-400i relies on the digital camera mounted on the top of the instrument to attribute color information to each pixel. However, the calibration data of the camera is required for this passage. While the internal calibration of the camera is known a priori, the external calibration must be recalculated whenever the camera is mounted on the instrument. External calibration parameters can be estimated by matching common points between the scan and the images acquired at the same station point. After this process, each point in the cloud is colored as the corresponding pixels of the assigned calibrated images. The georeferenced point cloud (Figure 3) was finally exported (.las format).



Figure 3: Point cloud views.

3.4 Image-based Acquisition and Processing

The following subsections describe the integrated approach to image-based acquisition and its processing.

3.4.1 The UAS Flight

The roofs were surveyed at high-resolution using a DJI Mini Mavic UAS. The captures were nadiral and oblique to cover the entire area and gather information about ceilings and walls to be integrated into the LiDAR model. The flight height was 40 m above the ground to obtain Ground Sample Distance (GSD) lower than 2 cm. Overall, 1599 images were acquired.

3.4.2 Close-Range Photogrammetric Acquisitions

Creating a virtual environment requires high-quality 3D model textures to ensure immersive user navigation. Acquiring digital images from the ground at high resolution was necessary to achieve a high-resolution texture of the facades of buildings. About 400 images were captured with a NIKON D800E camera and taken as nadiral as possible to the facades. The data collection interested the buildings overlooking the two squares and Carlo Alberto's statue. To enrich the virtual model and to make the navigation more realistic, the textures were also applied to the secondary interest areas (e.g., adjacent streets and entrances to buildings). Since many of these streets are narrow, a spherical camera was used to quickly capture large portions of the facades. Ninety-two spherical images were acquired within the area of interest with a Ricoh Theta V spherical camera, ensuring sufficient overlap with the data acquired by UAS and terrestrial images.

3.4.3 Photogrammetric Processing

All the photogrammetric data have been processed with Agisoft Metashape Professional, a commercial software based on SfM.

At first, the relative position between photos is reconstructed, performing a fully automatic alignment between images. In this phase, a first photogrammetric calibration of the camera is carried out to determine the correct focal distance, the position of the main point, the distortions of the sensor, and both radial and tangential optics. Subsequently, 10 GCPs were manually collimated on the various images; 5 were chosen and used as checkpoints (CPs). The block compensation is then resolved by obtaining the residuals on GCPs and CPs, and the camera calibration is refined. In the end, the images are correctly positioned and oriented in the space concerning the isometric coordinate system.



Figure 4: Dense point cloud.

3.5 Generation of the Textured 3D Model

To create the textured 3D model of the study area, i.e., a three-dimensional mesh, the dense point clouds obtained with the procedures described above have been integrated, creating a complete model of the urban environment. The dense cloud was subsampled into seven different portions to be processed separately, choosing a full resolution for the main buildings (Carignano Palace and the National Library) and Carlo Alberto's statue and 1 to 5 cm for buildings facing the square and terrain. The dense georeferenced models were used for the 3D mesh generation, setting a high-quality level that allows the generation of the maximum number of possible triangles (Figure 5). The only exception concerns Carignano Palace and the National Library, which have been further subdivided for each floor of the building to guarantee an optimal visualisation of the virtual model avoiding problems of platform overload. It was chosen to generate a mesh with the maximum number of triangles in the lower portions of the facades and to limit the quality of the model on the subsequent floors.

By knowing the external orientations and radiometric information of all images, it was possible to generate a high-resolution texture for each reconstructed mesh automatically. Not all images were used for texturing but only those acquired under uniform lighting conditions.



Figure 5: Example of textured mesh. Carlo Alberto’s statue (left) and Carignano Palace (right).

4 RESULTS AND DISCUSSION

4.1 The Terrestrial LiDAR Acquisitions

The accuracy of the scanning registering procedure is expressed in terms of the estimated deviations between the targets identified in the scans and their known coordinates (Table 2).

Table 2: Estimated residues between targets identified in scans and known coordinates measured by topographic technique.

| | dX [m] | dY [m] | dZ [m] | Dist. [m] |
|-------------|----------|----------|----------|-----------|
| Min | -0.08946 | -0.07368 | -0.13934 | 0.001692 |
| Max | 0.088073 | 0.105132 | 0.087002 | 0.156342 |
| Mean | 0.000671 | -0.00033 | 0.002233 | 0.032446 |
| RMSE | 0.018788 | 0.020184 | 0.029044 | 0.040049 |

As a result of the recording procedure, a single point cloud with about 5 billion points was generated (Figure 4). The result is a three-dimensional representation of the study area containing radiometric and LiDAR intensity information.

During LiDAR acquisitions, unnecessary data are often recorded. Especially in urban environments, raw scanning data are noisy due to interferences, such as high-reflective surfaces (i.e., headlights, water), transparent surfaces (i.e., glazing), and elements in motion (e.g., people, vehicles). The latter was the most intrusive noise source: during measurement operations, the pedestrians passing through the area generated noise in the clouds. This aspect can be considered a limitation in LiDAR technology, which needs a multi-sensor data integration approach in areas with a high tourist impact. At first, all the people and unnecessary objects in the scene were manually removed from the point cloud. Subsequently, the

residual noise was filtered using a Statistical Outlier Removal (SOR), which removes the points with a high probability of not belonging to the modelled surfaces. Specifically, it calculates the average distance of each point to a number of its neighbours (6 in this application). It removes the points farther than the average distance summed to the product of the standard deviation to a coefficient (0.5 in this application).

Despite the filtering operations, managing the point cloud was still tricky and time-consuming due to the high point density. Hence, the cloud was subsampled with respect to the area’s level of interest to facilitate the analysis and modelling processes.

4.2 Photogrammetric Processing

A statistical evaluation of the image processing output was conducted by analysing the estimated residuals on the control points and checkpoints (Table 3). The obtained values indicate the overall geometric accuracy of the photogrammetric models generated through the SfM approach.

Table 3: Results of the photogrammetric block adjustment.

| | X (m) | Y (m) | Z (m) |
|----------------------|-------|-------|-------|
| RMSE | 0.016 | 0.013 | 0.027 |
| 10 GCPs error | 0.019 | 0.017 | 0.022 |
| 5 CPs error | 0.016 | 0.013 | 0.027 |

Thus, the point cloud describes the roofs of the buildings and the volumes in elevation exhaustively. Still, it is rather sparse in the lower parts of the buildings in narrow streets that appear distorted also in oblique images. It was also decided to limit the number of photogrammetric acquisitions from the ground in these areas and to exploit LiDAR data for 3D reconstruction.

4.3 Textured Models

Table 4 shows the number of triangles describing the meshes of the final 3D model of the study area.

Table 4: Number of mesh triangles describing each main zones/objects in the study area.

| Surveyed object | Triangles |
|-------------------------------------|--------------|
| Statue | ~ 9,480,000 |
| Carignano Palace Facade | ~ 16,847,000 |
| National library | ~ 8,903,000 |
| Building in Carignano square | ~ 5,730,000 |
| Building in via via Principe Amedeo | ~ 7,170,000 |
| Building in via Cesare Battisti | ~ 15,990,000 |
| Terrain | ~ 432,000 |

4.4 Multi-Sensor and Multi-Scale Approach

Among the various obstacles encountered in generating the highly detailed 3D model, the difficult survey conditions significantly impacted the processing time. Indeed, the noise in the cloud caused by many pedestrians in the survey area (winter tourism peak) has been solved through a time-consuming manual intervention on the point clouds. The orientation of the data within the same reference system is the basis for a correct data fusion. Consequently, a thorough and extensive topographic survey proved to be fundamental for data integration and evaluation.

Regarding the partially shaded facades of tall buildings in narrow streets, the data acquisition was planned so that the illumination conditions were consistent throughout the model. However, the photogrammetric information from those areas is sparser due to the distortions generated when very tall (or long) elements are captured up close by an optical sensor. The reconstruction of the texture of the narrow streets was possible thanks to the spherical camera (Ricoh). In this regard, in line with the considerations of other authors, the results of this work demonstrate the complexity of the choice of sensors that requires knowledge about the operability of sensors in terms of resolutions, characteristics, and behaviour in specific operational fields. Thus, the analyst's role in identifying the correct combination of sensors according to the requested level of detail is crucial. When adequately planned, integrated approaches are successful solutions for constructing highly detailed 3D virtual models thanks to their customizability in terms of time, costs, and sensors. Through a careful combination of sensors and algorithms, final products with specific levels of detail can be obtained.

5 CONCLUSIONS

In this work, a 3D model of part of the historical centre of Turin was generated at a very high resolution to be used in different domains. Indeed, it is (i) the base for the design of a new station of the metro line, (ii) a digital memory of the square, and (iii) the database for a virtual reality model. The proposed LiDAR and SfM-MVS integrated approach to build a highly detailed 3D virtual model can be replicated in other urban and natural environments. However, although highly detailed 3D modelling is becoming more and more widespread, there are still

no general standard procedures for their generation. The geomatic community is moving to fill this gap. This work represents a step towards the standardization of operations. It emphasizes the importance of integrating geomatic techniques, but further studies on replicability in disparate urban environments must be investigated.

REFERENCES

- Biljecki, F., Stoter, J., Ledoux, H., Zlatanova, S., & Çöltekin, A. (2015). Applications of 3D City Models: State of the Art Review. *ISPRS International Journal of Geo-Information*, 4(4), 2842–2889. <https://doi.org/10.3390/ijgi4042842>
- Billen, R., Cutting-Decelle, A.-F., Marina, O., de Almeida, J.-P., M., C., Falquet, G., Leduc, T., Métral, C., Moreau, G., Perret, J., Rabin, G., San Jose, R., Yatskiv, I., & Zlatanova, S. (2014). 3D City Models and urban information: Current issues and perspectives: European COST Action TU0801. In R. Billen, A.-F. Cutting-Decelle, O. Marina, J.-P. de Almeida, C. M., G. Falquet, T. Leduc, C. Métral, G. Moreau, J. Perret, G. Rabin, R. San Jose, I. Yatskiv, & S. Zlatanova (Eds.), *3D City Models and urban information: Current issues and perspectives – European COST Action TU0801* (p. I–118). EDP Sciences. <https://doi.org/10.1051/TU0801/201400001>
- Chen, R. (2011). The development of 3D city model and its applications in urban planning. *2011 19th International Conference on Geoinformatics*, 1–5. <https://doi.org/10.1109/GeoInformatics.2011.5981007>
- Chiabrando, F., Sammartano, G., Spanò, A., & Spreafico, A. (2019). Hybrid 3D Models: When Geomatics Innovations Meet Extensive Built Heritage Complexes. *ISPRS International Journal of Geo-Information*, 8(3), 124. <https://doi.org/10.3390/ijgi8030124>
- El-Hakim, S. F., Beraldin, J.-A., Picard, M., & Godin, G. (2004). Detailed 3D reconstruction of large-scale heritage sites with integrated techniques. *IEEE Computer Graphics and Applications*, 24(3), 21–29. <https://doi.org/10.1109/MCG.2004.1318815>
- Jovanović, D., Milovanov, S., Ruskovski, I., Govedarica, M., Sladić, D., Radulović, A., & Pajić, V. (2020). Building Virtual 3D City Model for Smart Cities Applications: A Case Study on Campus Area of the University of Novi Sad. *ISPRS International Journal of Geo-Information*, 9(8), 476. <https://doi.org/10.3390/ijgi9080476>
- Kobayashi, Y. (2006). Photogrammetry and 3D city modelling. *Digital Architecture and Construction*, 1, 209–218. <https://doi.org/10.2495/DARC060211>
- Kocaman, S., Zhang, L., Gruen, A., & Poli, D. (2006). *3D City Modeling from High-resolution Satellite Images* [Application/pdf]. 6 p. <https://doi.org/10.3929/ETHZ-B-000158058>
- Lemmens, M. (2011). Terrestrial Laser Scanning. In M. Lemmens, *Geo-information* (pp. 101–121). Springer

- Netherlands. https://doi.org/10.1007/978-94-007-1667-4_6
- Nex, F., & Rinaudo, F. (2011). LiDAR or Photogrammetry? Integration is the answer. *Italian Journal of Remote Sensing*, 107–121. <https://doi.org/10.5721/ItJRS20114328>
- Pepe, M., Fregonese, L., & Crocetto, N. (2022). Use of SfM-MVS approach to nadir and oblique images generated through aerial cameras to build 2.5D map and 3D models in urban areas. *Geocarto International*, 37(1), 120–141. <https://doi.org/10.1080/10106049.2019.1700558>
- Püschel, H., Sauerbier, M., & Eisenbeiss, H. (2008). *A 3D Model of Castile Landenberg (CH) from Combined Photogrammetric Processing of Terrestrial and UAV based Images* [Application/pdf]. <https://doi.org/10.3929/ETHZ-B-000011989>
- Ramos, M. M., & Remondino, F. (2015). Data fusion in Cultural Heritage – A Review. *The International Archives of the Photogrammetry, Remote Sensing and Spatial Information Sciences*, XL-5/W7, 359–363. <https://doi.org/10.5194/isprsarchives-XL-5-W7-359-2015>
- Remondino, F., & El-Hakim, S. (2006). Image-based 3D Modelling: A Review: Image-based 3D modelling: a review. *The Photogrammetric Record*, 21(115), 269–291. <https://doi.org/10.1111/j.1477-9730.2006.00383.x>
- Rodríguez-González, P., Muñoz-Nieto, A. L., del Pozo, S., Sanchez-Aparicio, L. J., Gonzalez-Aguilera, D., Micoli, L., Gonizzi Barsanti, S., Guidi, G., Mills, J., Fieber, K., Haynes, I., & Hejmanowska, B. (2017). 4D Reconstruction and Visualization of Cultural Heritage: Analyzing our Legacy Through Time. *The International Archives of the Photogrammetry, Remote Sensing and Spatial Information Sciences*, XLII-2/W3, 609–616. <https://doi.org/10.5194/isprs-archives-XLII-2-W3-609-2017>
- Rottensteiner, F., Trinder, J., & Clode, S. (2005). Data acquisition for 3D city models from LIDAR: Extracting buildings and roads. *Proceedings. 2005 IEEE International Geoscience and Remote Sensing Symposium, 2005. IGARSS '05., 1*, 521–524. <https://doi.org/10.1109/IGARSS.2005.1526226>
- Sahin, C., Alkis, A., Ergun, B., Kulur, S., Batuk, F., & Kilic, A. (2012). Producing 3D city model with the combined photogrammetric and laser scanner data in the example of Taksim Cumhuriyet square. *Optics and Lasers in Engineering*, 50(12), 1844–1853. <https://doi.org/10.1016/j.optlaseng.2012.05.019>
- Sato, T., Kanbara, M., & Yokoya, N. (2003). Outdoor scene reconstruction from multiple image sequences captured by a hand-held video camera. *Proceedings of IEEE International Conference on Multisensor Fusion and Integration for Intelligent Systems, MFI2003.*, 113–118. <https://doi.org/10.1109/MFI-2003.2003.1232642>
- Singh, S. P., Jain, K., & Mandla, V. R. (2013). Virtual 3D City Modeling: Techniques and Applications. *The International Archives of the Photogrammetry, Remote Sensing and Spatial Information Sciences*, XL-2/W2, 73–91. <https://doi.org/10.5194/isprsarchives-XL-2-W2-73-2013>
- Smith, M. W., Carrivick, J. L., & Quincey, D. J. (2016). Structure from motion photogrammetry in physical geography. *Progress in Physical Geography: Earth and Environment*, 40(2), 247–275. <https://doi.org/10.1177/0309133315615805>
- Tse, R. O. C., Gold, C., & Kidner, D. (2008). 3D City Modelling from LIDAR Data. In P. van Oosterom, S. Zlatanova, F. Penninga, & E. M. Fendel (Eds.), *Advances in 3D Geoinformation Systems* (pp. 161–175). Springer Berlin Heidelberg. https://doi.org/10.1007/978-3-540-72135-2_10
- Wang, C., Wen, C., Dai, Y., Yu, S., & Liu, M. (2020). Urban 3D modeling with mobile laser scanning: A review. *Virtual Reality & Intelligent Hardware*, 2(3), 175–212. <https://doi.org/10.1016/j.vrih.2020.05.003>
- Wang, J., & Li, C. (2007). *Acquisition of UAV images and the application in 3D city modeling* (L. Zhou, Ed.; p. 66230Z). <https://doi.org/10.1117/12.791426>
- Westoby, M. J., Brasington, J., Glasser, N. F., Hambrey, M. J., & Reynolds, J. M. (2012). ‘Structure-from-Motion’ photogrammetry: A low-cost, effective tool for geoscience applications. *Geomorphology*, 179, 300–314. <https://doi.org/10.1016/j.geomorph.2012.08.021>
- Yalcin, G., & Selcuk, O. (2015). 3D City Modelling with Oblique Photogrammetry Method. *Procedia Technology*, 19, 424–431. <https://doi.org/10.1016/j.protcy.2015.02.060>
- Zhu, Q., Hu, M., Zhang, Y., & Du, Z. (2009). Research and practice in three-dimensional city modeling. *Geo-Spatial Information Science*, 12(1), 18–24. <https://doi.org/10.1007/s11806-009-0195-z>